Observation of temporal plasma-wave echoes in an ion-wave regime

N. Yugami, S. Kusaka, and Y. Nishida
Department of Electrical and Electronic Engineering, Utsunomiya University, 2753 Ishii-machi, Utsunomiya, Tochigi 321, Japan
(Received 19 August 1993)

Temporal echoes in an ion-wave regime are observed in microwave-plasma interaction experiments. When two short microwave pulses ($\tau \leq 1/f_{pi}$, where τ is the pulse width and f_{pi} is ion plamsa frequency) are applied successively, one after another, in the nonuniform magnetic-field-free plasma, waves in ion plasma frequency range and plasma density cavity (caviton) are excited at the critical layer of the resonance absorption. After the waves damp out by Landau damping, temporal echoes appear in both the critical layer and underdense region. In the overdense region, however, no echo appears in the present experiments. The results are explained by the theoretical prediction given by Gould, O'Neil, and Malmberg [Phys. Rev. Lett. **19**, 219 (1967)].

PACS number(s): 52.35.Fp, 52.35.Mw, 52.40.Nk

I. INTRODUCTION

Plasma-wave echoes were predicted for the first time by Gould and co-workers [1,2] more than two decades ago, and many of the experimental observations have been published on electron plasma waves by Malmberg *et al.* [3] and ion plasma waves by Ikezi and co-workers [4,5] and Baker and co-workers [6,7]. Therefore the "echo" phenomenon is not necessarily a very topical subject. The observed echoes so far, however, have been restricted to only *spatial phenomena* except for one report on the electron-cyclotron temporal echoes [8], although the original theoretical prediction was for both temporal and spatial echoes. The analogy between the spatial echoes and temporal ones seems to be appropriate, but the real phenomena are different from each other. In the spatial echoes, the key phenomenon is that the particles stream through the idealized two gates localized in different places, as in the schematic model given by Baker, Ahern, and Wong [6]. Here, the "gates" in the experiments are formed by the fluctuating potential of traveling waves. Therefore the spatial echoes seem to result from the partial scattering of plasma particles by two "gates," i.e., the plasma particles are modulated by the first "gate" and then the majority of the particles go through the second gate. Some of the modulated particles, however, could be absorbed by the second "gate" existing in a downstream spatial position. Therefore most of the particles which can go linearly through two gates meet at certain positions to reconstruct macroscopic electric fields. The position is determined by two modulation frequencies of the gate waves and the separation between two gates, the excitation location. If there are a large number of collisions between particles, their trajectories are randomly scattered, and no reconstruction of the macroscopic field occurs. The spatial echo phenomenon is essential to show evidence of the reversibility of the Landau damping process in space.

Even if the spatial echoes show evidence for the reversibility of the spatial Landau damping, they do not necessarily show the reversibility of the Landau damping process with respect to *time*. In the temporal echoes, the memory in the distribution function could play the key role, and the echo reconstruction in the time domain should really be the predicted phenomena of the memory in the distribution function which is modulated and deformed around the velocity coinciding with the phase velocity of the wave. The existence of the temporal echoes means that the wave damping can be reversible in time, and the irreversible process of particle collision, which destroys the memory of the distribution function, should be negligibly small.

The temporal echoes of the plasma wave have been observed so far only on the electron-cyclotron wave [8], to our best knowledge, and the present experiments show experimental observation of the temporal echo phenomena in an ion-wave regime.

It is convenient to review the theory given by Gould, O'Neil, and Malmberg [1]. At first, a wave with a wave number k_1 is excited at $t=0$, which is damped away within certain time duration δ_1 by the Landau damping, and then at $t=t_1$ ($>\delta_1$), another wave is excited with a different wave number k_2 or frequency ω_2, and smeared out completely in its phase. At a certain time t_2 ($>t_1$) after the second wave has damped away within a time duration δ_2 ($<t_2-t_1$), a macroscopic electric field of the wave can be reconstructed even if there is no forced excitation at this stage, t_2. This is called an echo. When the echo is reconstructed, there is a relationship between two characteristic times and wave numbers as follows [1]:

$$t_2=\frac{k_2}{k_2-k_1}t_1 \ . \tag{1}$$

If wave dispersion is assumed weak, Eq. (1) can be rewritten as

$$t_2=\frac{\omega_2/c_2}{\omega_2/c_2-\omega_1/c_1}t_1=\frac{\tau_1}{\tau_1-\tau_2}t_1 \ , \tag{2}$$

where $c_{1,2}$ are the speed of waves in the ion plasma frequency range, and are different from each other, in general, between two waves, and $\omega_{1,2}=2\pi/\tau_{1,2}$ are wave fre-

quencies. If velocities of two waves are almost identical, $c_1 \approx c_2$, the final result in Eq. (2) is obtained. This could be allowed in most of the cases as far as the present experiments are concerned.

II. EXPERIMENTAL SETUP

The present experiments are performed in a nonuniform argon plasma confined to a stainless steel chamber which is 60 cm in diameter by 1 m long, the wall of which is covered with many multidipole permanent magnets [9] (see Fig. 1). The magnetic pole faces in each row pointed in the same direction. The rows alternated in magnetic pole orientation, creating the magnetic barrier necessary to contain the plasma.

The vacuum chamber is evacuated to a pressure lower than $p \approx 1 \times 10^{-6}$ Torr. Typical plasma parameters are a maximum electron density $n_e \leq 2 \times 10^{11}$ cm^{-3}, an electron temperature $T_e \approx 3$–5 eV, and an ion temperature $T_i \approx \frac{1}{10} T_e$ in a neutral argon gas with pressure $p \approx 4 \times 10^{-4}$ Torr. Here, ionizing electrons from the Th-W filaments are accelerated by bias voltages up to 110 V, applied between filaments and anode (chamber wall), which is grounded. Typical density gradient scale length in the axial direction is $L = (d \ln n_e / dz)^{-1} \approx 80$–$100$ cm. Here, the plasma parameters and wave signals are measured by Langmuir probes made of a semirigid coaxial cable with a probe tip of 0.1 mm diameter by 0.5 mm length. The probes are movable in the axial direction (z direction) and rotatable in the radial direction, so that we can measure spatial profiles of both axial and radial directions. When density fluctuations are measured, the probe is biased slightly into the electron saturation current region (≈ 40 V against the ground potential). All the signals are analyzed by using a computerized storage system with boxcar averaging system and/or on the oscilloscope screen.

A microwave with frequency $f_0 = \omega_0 / 2\pi = 2.86$ GHz and maximum power of 10 kW is irradiated through a high gain horn antenna (about 17 dB gain) installed in the lower-density side. The antenna has a metallic microwave lens in front of it. The critical density layer for the resonance absorption [9–12] is located around the middle of the chamber, i.e., $z = 22$–25 cm measured from the microwave-lens edge. This location, however, depends on the experimental conditions, and can be adjusted in a desired position. A width of the microwave pulse employed in this experiment is typically of 50–70 nsec at fullwidth at half maximum (FWHM) with a repetition of 10 Hz. Acrylic resin board is used for the chamber wall at the far end of the chamber from the horn antenna, and the wall behind the horn antenna is covered with stainless steel rags; all of these facilities are for the purpose of minimizing the reflection effect of the scattering microwave within the chamber.

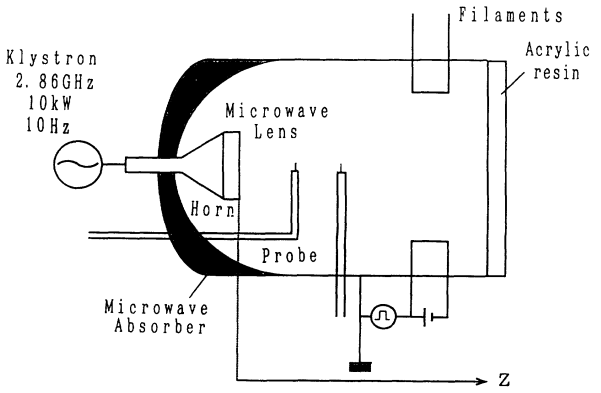

FIG. 1. Experimental apparatus.

III. EXPERIMENTAL RESULTS

A. Single pulse excitation

When a narrow rf pulse is irradiated, a large-amplitude electron plasma wave can be excited at the critical layer where $\omega_0 = \omega_{pe}$ is satisfied. Here, ω_{pe} is the frequency of the electron plasma wave at the critical layer. A typical

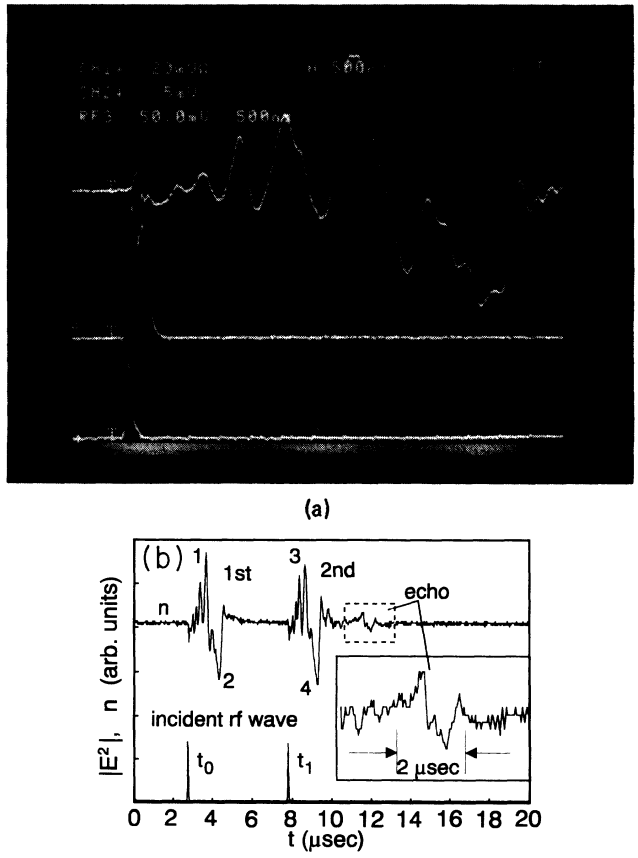

FIG. 2. Typical wave forms excited by short microwave pulses. (a) Oscilloscope trace of the electron-density fluctuation is in top trace, the envelope of high-frequency electric-field fluctuation, $|E^2|$ ($f \geq 10$ MHz), is in middle trace, and the shape of incident microwave pulse is in bottom trace. (b) The trace of wave form and echo observed in electron-density fluctuation (the probe is biased in 40 V) are in top trace and the applied rf pulse is in bottom trace. Inset shows the enlarged figure of the echo.

wave form observed at the critical layer is shown in Fig. 2(a). Here, the top trace shows electron-density fluctuations, the middle trace shows electric-field fluctuations measured through the crystal detector, and the bottom trace refers to the incident microwave pulse. Note that the present detector employed for measuring the electric-field fluctuation has a frequency response of 0.01–18 GHz (model HP-463), so that low-frequency electric-field fluctuations caused by the waves with frequency in the ion-wave regime were not detected, but only the envelope of the electron plasma-wave was. When an observation point was shifted down along the density gradient toward the horn antenna, almost the same wave forms were observed. In the overdense region, however, this instability disappears in a short spatial duration. Large-amplitude electron plasma waves, shown in the middle trace, run down along the plasma density gradient. At the same time, high-energy electron emission ($\epsilon > 50$ eV, where ϵ is the maximum energy) was observed as well within this duration (not shown here). The electrons have been shown to be accelerated by large-amplitude electron plasma waves excited near the critical layer, and also run down along the density gradient very quickly. Here, the incident microwave pulse should be of the width of about one ion plasma-wave period or less, otherwise the present wave cannot be excited. A bunch of electrons could be pushed out by the ponderomotive force of the electromagnetic wave localized near the critical layer. After turn off of the microwave pulse the positive space charge remains there, and the resultant ambipolar Coulomb force can drive ion waves. Thus the traveling electron bunch could excite the wakefield in the ion-wave regime successively in space. This situation is quite similar to the previous results [13], in which a bunch of ions was employed to excite the ion-wave wakefield. Therefore the wave velocity should be very close to the traveling velocity of the electron bunch.

We also recognize that there is a lower-frequency component in the wave form. This is essentially the envelope of the higher-frequency component. This part of the wave is the density streamer which is excited as a density deformation due to the ponderomotive force of the high-frequency soliton, i.e., the electric-field pressure digs a hole at the critical layer, and the initial critical density layer is pushed up toward both the higher- and the lower-density side. The finite strength of the accumulated field energy is balanced by the plasma pressure, resulting in a cessation in the deformation of the density profile. This occurs after the rf power is turned off, because of large inertia of ion mass, and ion-wave streamers which have velocity determined by the balance between the bunch of electrons and the excited waves begin to propagate from this position. Thus we can say that the low-frequency wave is the envelope of the present high-frequency waves, and that is essentially the same kinds of cavities which have already been observed so far [9–12]. However, the high-frequency waves have never been observed in the past experiments. The precise characteristics of these waves are out of the present scope and will be published elsewhere [14].

B. Double pulse excitation

We have tried double pulse excitation of the present wave, in order to excite the wave with much larger density fluctuations. When two microwave pulses are irradiated at separate times, the same kind of waves can be excited at each time. Here, the excitation principle may follow the next relationship,

$$\frac{d^2 n_1}{dt^2} + \omega_0^2 n_1 = A_0 \delta(t - t_1) , \tag{3}$$

where $n_1 \equiv \delta n / n_0$ $(t = t_0)$ is the density fluctuation excited at $t = t_0$, and A_0 is the wave amplitude excited at $t = t_1$. Here, t_1 was varied with respect to t_0; the time when the first microwave pulse is irradiated. A typical example of the wave forms is shown in Fig. 2(b). This is observed at the critical layer $z \approx z_c$ (≈ 21.5 cm). Note that the temporal echo is observed in later time of enough separation from two rf pulses. The echo phenomena will be discussed later. Here, each peak of the waves is labeled as 1–4, as shown in Fig. 2(b).

If the wave is observed in the underdense region ($z < 22$ cm), the excited waves by the second pulse, denoted as 1 and 2 [see Fig. 2(b)], become maximum in amplitude around $t_1 - t_0 \approx 1.5$ μsec, while the waves labeled 3 and 4 do not increase at all, as shown in Fig. 3(a). For enough separation of two incident microwave pulses, such as $t_1 - t_0 \geq 4$ μsec, the waves 1, 2, 3, and 4 are independently excited with amplitude $\delta n / n_0 \approx 20\%$. The maximum amplitude of all the waves excited by the forced excitation reaches about 35–40 %, but it has never

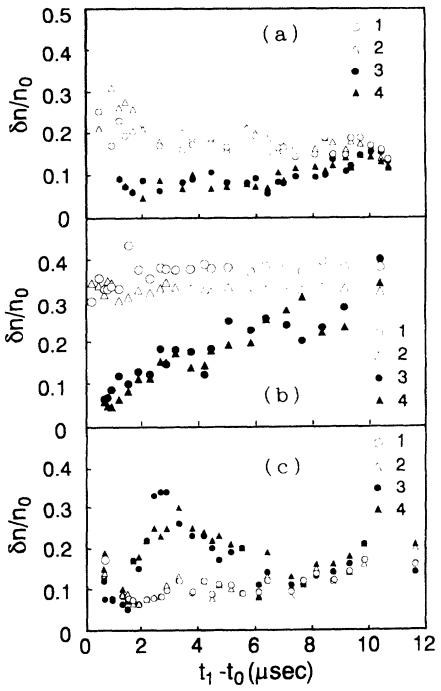

FIG. 3. Double pulse excitation of the wave, measured (a) in the underdense region, (b) at the critical layer, and (c) in the overdense region.

become larger than this value.

When the same phenomena were observed at the critical layer where $n_0 \approx n_c$ ($z_c = 21.5$ cm), the results change slightly, as shown in Fig. 3(b). In this case, the waves excited by the first pulse, denoted as 1 and 2, always have large amplitude of 35–40 % throughout the entire time difference $t_1 - t_0$, up to 10 μsec, while the waves excited by the second pulse become gradually larger with $t_1 - t_0$, and reach about 40%, when there is no interference with the first bunch of waves.

In the overdense region ($z \approx 23$ cm), however, the phenomena change drastically, as shown in Fig. 3(c). The maximum amplitude of the waves in this case can again reach about 30% by forced excitation of two pulses at $t_1 - t_0 \approx 3$ μsec, but these are 3 and 4, not 1 and 2. Enough separation of two pulses makes the wave amplitude smaller by about 20%. From all of these results we failed to excite the wave with much larger amplitude than about 40%. Even in a single pulse excitation we have observed the wave with amplitude of 40%. Therefore we have to conclude on this phenomenon that the maximum amplitude of the wave is determined by the characteristic nature of the present wave itself and plasma parameters, not the excitation method.

C. Observation of temporal echoes

After two waves damped out, temporal echoes in an ion-wave frequency regime have been observed at a certain time after the second wave smeared out in the phase; an example is shown in Fig. 2(b). Here, the second pulse should be applied after the wave excited by the first pulse damped out completely.

Examples of the spatial distribution of the excited waves and echoes are shown in Fig. 4, where the electron-density fluctuations are illustrated. As clearly seen from this figure, two kinds of ion waves can be excited by the short microwave pulses. Immediately after the microwave irradiation is shut off, higher frequency with an even lower-amplitude wave starts oscillation, and shortly later, after the microwave pulse is turned off, the lower-frequency ion wave with large amplitude ($\delta n / n_0 \approx 40\%$ in the present case) can be excited.

The time when echoes are observed depends on the time interval of two microwave pulses; as the time interval becomes larger, the echo appears in later time; an example is shown in Fig. 5. The empirical relationship of $t_1 - t_0$ vs $t_2 - t_0$ is obtained as

$$t_2 - t_0 = K(t_1 - t_0) , \tag{4}$$

where $K = 1.6$–1.7 is observed. Comparing the experimental results with the theoretical prediction of Eq. (1), two wave numbers are obtained as $k_1 = 1.2$–1.3 cm^{-1}, and $k_2 = 3.2$–3.3 cm^{-1}. If we look at the experimental results shown in Fig. 4, we may recognize that typically two kinds of waves exist, as mentioned above; one has lower frequency of typically $f_L \approx 0.5$–0.6 MHz and the other has higher frequency of $f_H \approx 1.2$ MHz. The propagation velocities of two waves change by the same amount spatially to have a relationship $c_1 = c_2$

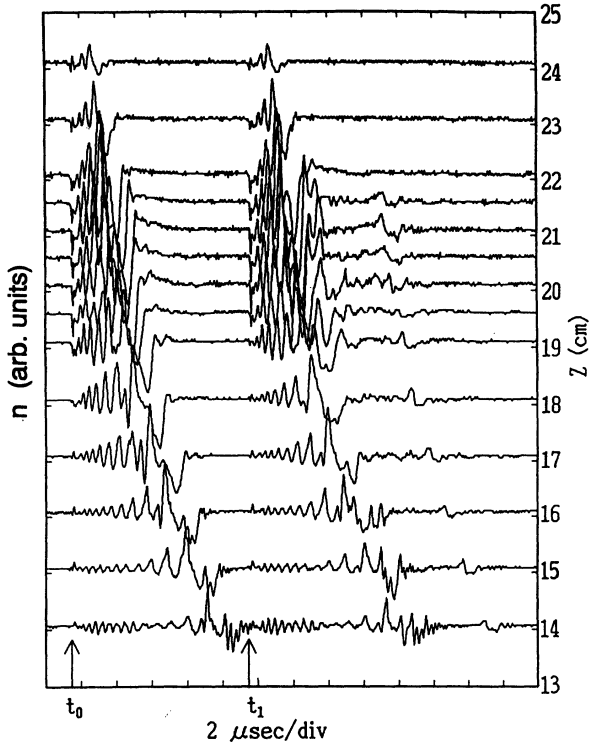

FIG. 4. Spatial distributions of wave forms in electron-density fluctuations. The resonance absorption layer is at $z \approx 21.5$ cm, and $t_1 - t_0 = 10$ μsec. Bias voltages on the probe are kept at 40 V, which is measured from the ground.

$= v_0 \exp(z/z_0)$, where $v_0 = (3.3 \pm 0.75) \times 10^6$ cm/sec, and $z_0 = 2.8 \pm 0.5$. Therefore we may use a typical value of $c_{1,2} \approx 3.5 \times 10^6$ cm/sec when the echoes appear dominantly. Here, the spatial location z is measured from the critical layer z_c which is located typically 21.5 cm from the horn antenna edge in the present experimental conditions.

We have never observed echoes in the overdense region ($z > z_c$), even if density cavities such as are seen in Fig. 4 have been observed. There is a clear cut between underdense and overdense boundary for echo appearance. This fact suggests that propagating high-frequency waves have

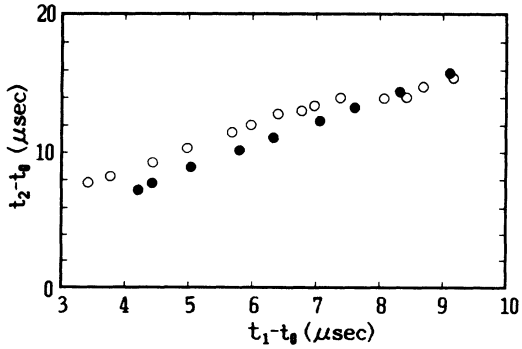

FIG. 5. The dependence of $t_2 - t_0$ on $t_1 - t_0$, where echo appears at t_2. Closed circles are measured at $z = z_c$ (≈ 21.5 cm) and open circles are in underdense region at $z \approx 20.5$ cm.

never been excited in the overdense region, because in this region the microwave is cut off and short pulse microwave propagation is inhibited. Furthermore, enough high-energy electrons may not be ejected into the overdense side, which is necessary for exciting high-frequency waves of the ion-wave regime, although a small number of high-energy electrons are observed in this region.

When we make the microwave pulse wider up to about 0.5–1.0 μsec or more, the high-frequency component of the wave disappears and only the lower-frequency density cavity mode (or ion-wave streamer) can be excited. In this situation the echo never appears even when two microwave pulses were applied to excite waves at the critical layer or in the underdense region.

The echo amplitudes are observed as a function of the position along the plasma axis, as shown in Fig. 6. In this example, the pulse interval t_1-t_0 is kept constant at 10 μsec. Here, a solid line in the figure shows the result fitted to data points. The amplitudes seem to fluctuate periodically with a "wavelength" of about 3 cm. As mentioned above, two kinds of waves exist in the present condition; one has a frequency of about 0.5–0.6 MHz and the other has higher frequency, of about 1.2 MHz. Therefore corresponding wavelengths are 5 and 2 cm, respectively. If we make a spatial beat wave, the wave number must be $k_- = k_2 - k_1 \approx 2.0\ \mathrm{cm}^{-1}$, which gives a corresponding wavelength $\lambda_- \approx 3$ cm. Therefore it is possible to make a spatial beat with two waves, which could modulate echo amplitude. This length should coincide with the value of typical wave velocity times echo period, i.e., the wavelength is $\lambda \approx c_1 \times 0.8\ \mu\mathrm{sec} \approx 2.9$–$3.5$ cm.

The echo amplitude changes with incident microwave power as shown in Fig. 7, which was observed at the critical layer and the pulse interval of two waves was again kept at 10 μsec. As you may see from the figure, the echo amplitude increases linearly with incident rf power up to 2 kW. Over this value the amplitude saturates as rf power, with the maximum amplitude of about 6%, or even some periodic fluctuations are observed.

IV. DISCUSSION

In the preceding section, we interpreted that the present instability is excited by the ponderomotive force

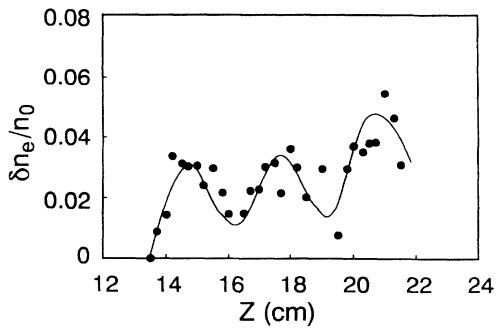

FIG. 6. The amplitude change of the echoes in space with $t_1-t_0=10$ μsec. The critical layer locates around $z=21.5$ cm.

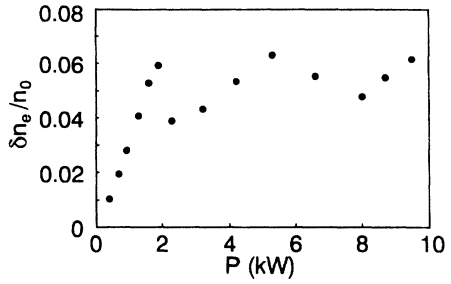

FIG. 7. Power dependence of the echo amplitude $\delta n_e/n_0$ with $t_1-t_0=10$ μsec measured at the critical layer ($z\approx 21.5$ cm).

of the rf field. However, there is a discussion that the high-frequency part of the wave may be the "ballistic mode" [15]. If we assume that the electron bunch travels down the plasma along its density gradient from the critical layer, the velocity v_b of the ballistic mode could be determined in this case by the stream velocity of the bunch. Here, $v_b=\sqrt{2eV/m_e}$, and V is the voltage difference for electron acceleration measured from the plasma potential. Therefore the acceleration voltage of the bunch would be about $V\approx 35$ V. This is a reasonable amount created at the critical layer, and the cavity in the present experiment may seem to be the ballistic mode, *at a glance*. However, the electron bunch is terminated quickly, with almost the same rate or less than the wave period of about 60 nsec. After the termination of the bunch, there is no electron flow or bunch flow at all. This fact reveals that there is no possibility of the ballistic mode, rather a wakefield is excited in the ion-wave regime. In Ref. [13], it is shown that a bunch of ions can excite the wakefield in the ion-wave regime. In the present experiments, however, a bunch of electrons, which result from the hot electron component, can excite the wakefield in almost the same regime.

Doubt may arise in that the detection probe may affect or excite the present wave. We have carefully checked the effects from the existence of probes to the present instabilities. The results show that moving the probe close to or away from the resonance layer did not affect the excitation amplitude or the wave form at all. Probe impedance and the signal processing circuit are also checked precisely to be sure they do not affect the excitation phenomena of the wave. All of these results give the conclusion that there are no serious effects from the detection probe to the wave phenomena.

The echo amplitudes, $\delta n_e/n_0$, attenuate exponentially with a time delay (t_1-t_0); an example is shown in Fig. 8. Here, the amplitude is measured either in the critical layer as shown in Fig. 8(a) or in the underdense region shown in Fig. 8(b). The open circles in the figure correspond to the positive side of the wave form of the echoes and the closed ones to the negative side. From these results, we can obtain the damping constant of typically 4.5 ± 0.4 μsec, which is roughly five times the typical oscillation period of the echo. This means that the damping of the echo is fairly weak and its amplitude does not change very much within the present experimental condi-

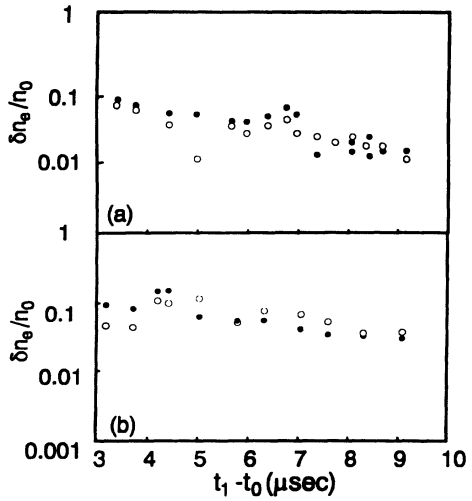

FIG. 8. The echo amplitude $\delta n_e/n_0$ as a function of $t_1 - t_0$, measured at (a) $z \approx z_c$ ($=21.5$ cm) and (b) $z \approx 20.5$ cm. Open circles refer to the positive side of wave forms of the echo and closed ones to the negative side.

tions. However, there is still damping of the echo amplitude. The damping of the echo may possibly be due to collisional damping which should be weak in order not to destroy the memory of the distribution function, otherwise the creation of echoes does not occur. The collision frequencies [16] between typical electron-electron or electron-ion collisions, ν_{ee} or ν_{ie}, in the present case become, respectively, $\nu_{ee} \approx 450$ kHz and $\nu_{ie} \approx 180$ kHz; corresponding collision times are 2.2 and 5.6 μsec, respectively. Therefore these collisions do not work for destroying the memory of the distribution function. If we look at the electron–neutral-species collision, on the other hand, the typical collision frequency ν_{en}, estimated from the published data [17], is given as $\nu_{en} \approx 1-2$ MHz ($1/\nu_{en} \approx 0.5-1$ μsec). The ion–neutral-species collision frequency ν_{in}, on the other hand, ranges about 50–70 kHz, corresponding mean collisional time is 14–17 μsec. From the above-mentioned results, we may conclude that the electron-neutral collision is the key damping mechanism of the echo amplitude. We, however, have not undertaken precise investigations yet, specifically of changing the damping rate of the echoes, because only small-amplitude echoes have been found so far, and it is not easy to excite large-amplitude ones.

V. CONCLUSION

The temporal plasma-wave echoes in ion-wave regime have been observed in the microwave-plasma interaction experiments. When the microwave pulse with width almost the same as or less than the ion plasma-wave period is applied, two kinds of large-amplitude waves with frequencies in the ion plasma-wave regime can be excited. The maximum amplitude of waves reaches about 40%. If two microwave pulses are applied successively one after another, the forced excitation of the wave can be observed, but its maximum amplitude is still less than about 40%. After two waves are damped out completely by the Landau damping process, the temporal plasma-wave echoes have been observed in the time domain. This could result from the modulation of the electron distribution function at the velocity close to the wave phase velocity. The electron–neutral-species collision is the key damping mechanism of echo amplitude in the present experiments.

ACKNOWLEDGMENT

This work was supported in part by the Grant-in-Aid for Scientific Research from the Ministry of Education, Science and Culture, Japan.

[1] R. W. Gould, T. M. O'Neill, and J. H. Malmberg, Phys. Rev. Lett. **19**, 219 (1967).
[2] T. M. O'Neil and R. W. Gould, Phys. Fluids **11**, 134 (1968).
[3] J. H. Malmberg, C. B. Wharton, R. W. Gould, and T. M. O'Neil, Phys. Rev. Lett. **20**, 95 (1968); Phys. Fluids **11**, 1147 (1968).
[4] H. Ikezi and N. Takahashi, Phys. Rev. Lett. **20**, 140 (1968).
[5] H. Ikezi, N. Takahashi, and K. Nishikawa, Phys. Fluids **12**, 853 (1969).
[6] D. R. Baker, N. R. Ahern, and A. Y. Wong, Phys. Rev. Lett. **20**, 318 (1968).
[7] A. Y. Wong and D. R. Baker, Phys. Rev. **188**, 326 (1969).
[8] R. M. Hill and D. E. Kaplan, Phys. Rev. Lett. **14**, 1062 (1965).
[9] Y. Nishida and T. Shinozaki, Phys. Rev. Lett. **65**, 2386 (1990), and references therein.
[10] Y. Nishida, A. Lee, N. C. Luhmann, Jr., and M. Rhodes, Plasma Phys. Cont. Fusion **32**, 391 (1990).
[11] Ann Lee, Y. Nsihida, N. C. Luhmann, Jr., S. P. Obenschain, B. Gu, M. Rhodes, J. R. Albritton, and E. A. Williams, Phys. Rev. Lett. **48**, 319 (1982).
[12] Ann Lee, Y. Nishida, N. C. Luhmann, Jr., C. Randall, M. Rhodes, and S. P. Obenschain, Phys. Fluids **29**, 3785 (1986).
[13] Y. Nishida, T. Okazaki, N. Yugami, and T. Nagasawa, Phys. Rev. Lett. **66**, 2328 (1991).
[14] Y. Nishida, S. Kusaka, and N. Yugami, Phys. Scr. (to be published).
[15] I. Alexeff, W. D. Jones, and K. E. Lonngren, Phys. Rev. Lett. **21**, 878 (1968).
[16] See, for example, F. F. Chen, *Introduction to Plasma Physics and Controlled Fusion*, 2nd ed. (Plenum, New York, 1988), Vol. 1.
[17] S. C. Brown, *Basic Data of Plasma Physics, 1966*, 2nd ed. (MIT Press, Cambridge, MA, 1967).

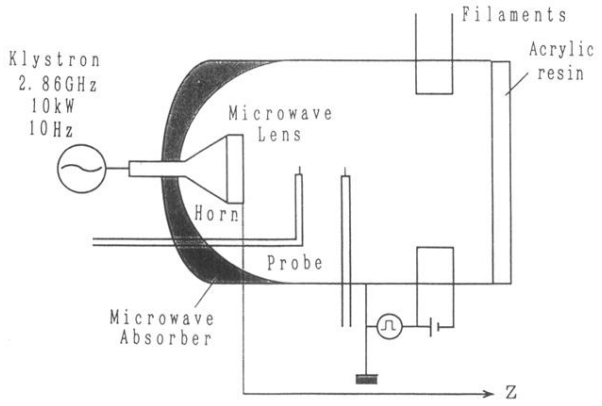

FIG. 1. Experimental apparatus.

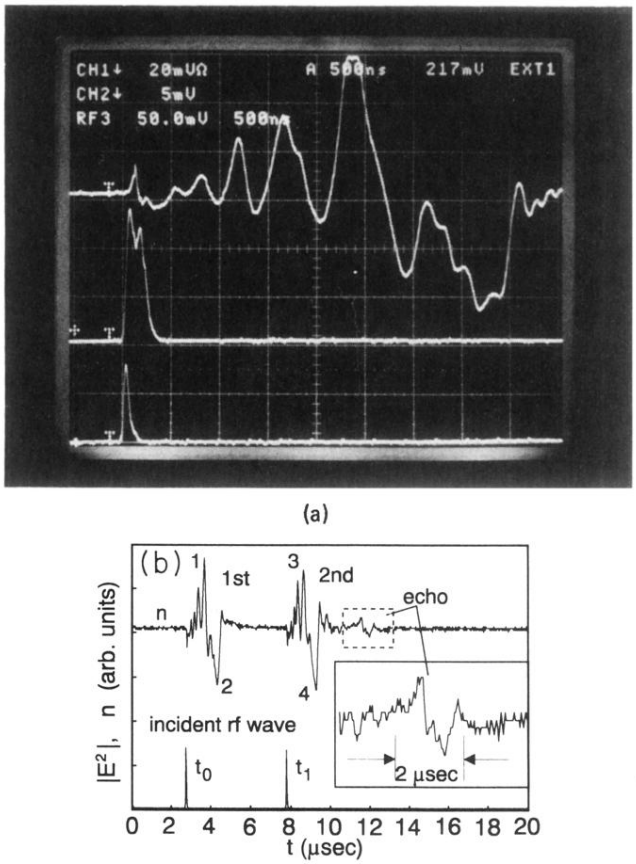

FIG. 2. Typical wave forms excited by short microwave pulses. (a) Oscilloscope trace of the electron-density fluctuation is in top trace, the envelope of high-frequency electric-field fluctuation, $|E^2|$ ($f \geq 10$ MHz), is in middle trace, and the shape of incident microwave pulse is in bottom trace. (b) The trace of wave form and echo observed in electron-density fluctuation (the probe is biased in 40 V) are in top trace and the applied rf pulse is in bottom trace. Inset shows the enlarged figure of the echo.